On the Evaluation of the Shielding Effectiveness of an Electrically Large Enclosure

Angelo Gifuni[1], Antonio Sorrentino[1], Alessandro Fanti[2*], Giuseppe Ferrara[1], Maurizio Migliaccio[1], Giuseppe Mazzarella[2], and Federico Corona[1]

[1]Dipartimento per le Tecnologie, Università degli Studi di Napoli Parthenope,
Centro Direzionale Isola C 4, Napoli, Italy
[2]Dipartimento di Ingegneria Elettrica ed Elettronica Pad. B, Università degli Studi di Cagliari
Piazza d'Armi 09123 Cagliari, Italy
*Alessandro Fanti, E-mail: alessandro.fanti@diee.unica.it

Abstract

The shielding effectiveness (SE) has become a fundamental step in testing active or passive electric devices. The Reverberating Chamber (RC) is a well-established method for determining the SE since has the advantage to expose the material to a more realistic environment. In this paper the SE_e of electrically large enclosures with a metallic mesh grid in a RC is evaluated. Enclosures made with metallic mesh are considered. In particular, it is shown that the SE of a material is unable to provide complete information for the SE_e of an electrically large enclosure made with the same material. Moreover, this latter one is related to the loading conditions within the enclosure itself. Measurements accomplished at RC of the Università di Napoli Parthenope (formerly Istituto Universitario Navale, IUN) confirm the physical soundness of the proposed approach.

1. Introduction

The importance of electromagnetic interference (EMI) and electromagnetic compatibility (EMC) in daily environment arises from the fact that the environment is electromagnetically hostile. The increasing use of electronic devices makes the EMI and EMC issues of great relevance in such environments in which more devices are used in disparate contexts. The enclosure are great of importance for controlling the emission of such electronic systems. On the other hand, they increase immunity of the devices subject to strong electromagnetic interference. A measure of the efficiency of an enclosure is the shielding effectiveness (SE_e), i.e. the ability of attenuating the sources of electromagnetic disturbance. Usually, the nested reverberating chamber (RC), with the mode-stirred method, is employed to characterize the enclosures [1-2]. Nested RCs have been used in the past to determine the SE of material [3]. The RC is an electrically large chamber which uses several stirring techniques to randomize the input electromagnetic field in order to expose the device under test to a more realistic environment [1].

The SE_e of an enclosure is defined as follows [1-2]

$$SE_e = -10\log_{10}\left(\frac{P_{in}}{P_{out}}\right) \quad (1)$$

where P_{in} is the power received by the receiving antenna placed in RC and P_{out} is the power received by a receiving antenna placed in the enclosure. Therefore, the SE_e relates the interior fields to the external incident field. The SE_e is a fundamental step in establishing the EMC of active or passive devices.

Among the different enclosures used to shield the electronic devices, the metallic meshes are potentially attractive as electromagnetic shield enclosure because of their reduced weight per unit area compared to metallic box. However, the metallic mesh often forms parts of enclosures, as it allows the aeration of the electronic circuits, which are shielded by enclosures themselves. The electromagnetic behavior of wire meshes has been previously addressed in [4-5].

In this paper, an electrically large enclosure is placed in an RC and measurements of the SE_e are accomplished. This type of configuration is essentially a nested RC [3, 6]. Clearly, the walls of the enclosure are regarded as reciprocal walls. In Fig.1 is shown a sketch of the measurement set-up. The field within the RC is well randomized by three stirrers. The set-up includes two antennas in the RC and a small monopole probe, which is placed on one interior wall of the enclosure. In Section 3, the experimental set-up is further discussed. Being the walls made of metallic mesh, the enclosure within the RC has no stirrers inside since all points into the enclosures statistically have the same fields level; The enclosure within the RC has no paddles since its mode density is quite high. As long as the SE_e is weak or moderate , the Q of all enclosure modes is low and each of those modes is randomly excited from the RC field. Therefore the internal field, is sum of all enclosure modes, is effectively randomized. In other words, the RC mode stirrers act as mode stirrer also for the enclosure. Following the

mathematical model developed in [7] this paper shows that the SE_e of the enclosure is smaller than that obtained by the same material exposed to an RC electromagnetic field. Further, the SE_e is dependent on the loading conditions of the enclosure. Measurements accomplished at RC of the Università di Napoli Parthenope (formerly Istituto Universitario Navale, IUN) confirm the physical soundness of the proposed approach and its applicability from an operational point of view.

2. Mathematical Model

In this section, two equivalent mathematical models for SE_e, based on power balance, are shown. An approach followed for measuring the SE_e of electrically large enclosure is based on the RC technique. It is assumed that the field is uniform and isotropic inside and outside the enclosure. Following the power balance theory, the SE_e of an electrically large enclosure can be expressed as follows [1-2]

$$\mathrm{SE_e} = 10\log\left(\frac{4\pi V}{\langle\sigma_t\rangle\lambda Q}\right) \tag{2}$$

where V and Q are the volume and the quality factor of the enclosure, respectively, λ is the working wavelength, and σ_t is the average transmission cross section (TCS) of the enclosure walls. $\langle\ \rangle$ represents the averaged over an incident angle of 4π steradians and over all polarizations.

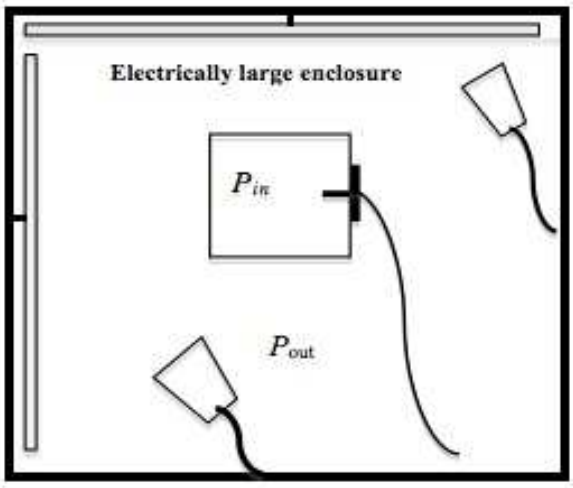

Figure 1: Illustration of the RC set-up measurements

From power balance it can be written [7]:

$$(S_o\sigma_t - S_i\sigma_t) = S_i(\sigma_{w,i} + \sigma_{a,i} + A_e) \tag{3}$$

whence [7]

$$\mathrm{SE_e} = \frac{P_{out}}{P_{in}} = \frac{\sigma_t + \sigma_{w,i} + \sigma_{a,i} + A_e}{\sigma_t} \tag{4}$$

where S_i and S_o are the incident power density inside and outside the enclosure, respectively; $\sigma_{w,i}$ is the total average absorption cross section (ACS) of the enclosure wall when the field impinges from the inner, $\sigma_{a,i}$ is the average ACS of the load, A_e is the effective area of the receiving antenna inside the enclosure [2], and σ_t is the one in eq. (2). It is important to note that in (4) SE_e is defined to be greater than 1 as in [1].

It must be noted that the trend of SE_e given by eq. (2), for different frequency range is not straightforward to draw, particularly for enclosure where σ_t is very sensitive to the frequency changes. Further, Q factor in eq. (2) is inversely proportional to σ_t. Equation (4) improves the comprehension of the SE_e of an enclosure; by setting

$$\sigma_{ae,i} = \sigma_{w,i} + \sigma_{a,i} + A_e \tag{5}$$

eq. (4) becomes

$$\mathrm{SE_e} = \frac{\sigma_t + \sigma_{ae,i}}{\sigma_t} \quad . \tag{6}$$

If the enclosure is unload, i.e. $\sigma_{a,i} = 0$, then

$$\sigma_{ae,i} = \sigma_{w,i} + A_e \quad . \tag{7}$$

In the case of a metallic mesh enclosure, the behavior of SE_e can be simply described by observing that the transmission cross section grows more rapidly with increasing of the frequency respect to $\sigma_{ae,i}$. In particular, at low frequencies, σ_t is smaller than $\sigma_{ae,i}$,. Hence, a SE_e greater than 1 is expected. On the other hand, as the frequency gradually increases, the transmission cross section increases faster than $\sigma_{ae,i}$. Therefore, a value of SE_e about equal to 1 (0 dB), is obtained. Accordingly, a decreasing trend of SE_e, with frequency is expected. In [7], it is shown that SE_e can be expressed as follows

$$\mathrm{SE_e} = \mathrm{SE}(1-\mathrm{R}) + \frac{\mathrm{A_e}}{\sigma_t} \tag{8}$$

where $\sigma_{a,i}$ has been assumed equal to zero; SE is the shielding effectiveness of the wall material; R is the reflectivity of the enclosure walls when the field impinges from the inner of the enclosure [8]. σ_t can be expressed as follows [7]

$$\sigma_t = \frac{\sigma_{t,gA}}{\mathrm{SE}} \tag{9}$$

where $\sigma_{t,gA}$ is the TCS of the total geometric area of the wall enclosure when they are considered perfectly

transmitting; clearly, σ_t is attendant to the same geometric area. The SE can be achieved as follows [7]:

$$\frac{1}{\mathrm{SE}} = (1-\mathrm{R}) - \frac{\sigma_{\mathrm{w,i}}}{\sigma_{\mathrm{a,gA}}} \qquad (10)$$

where $\sigma_{a,gA}$ is the total geometric area of the enclosure walls when they are considered perfectly absorbing [7]. It is important to note that $\sigma_{a,gA} \cong \sigma_{t,gA} = S_g/2$ where S_g is the surface area of enclosure walls. One specifies that in (9) SE is defined to be greater than 1.

Although the losses were negligible by setting $\sigma_{w,i}=0$ in eq. (10), pioneering results about R (SE) of metallic mesh grids have been carried out in [9].

In this paper, initial results of SE_e are predicted by using (8)-(10) and R measurements [9]; a comparison with measured SE_e is shown as well.

3. Experiment Results

In this section, a meaningful set of experimental results is shown. Before that, a brief description of the calibration procedure is first summarized. For the evaluation of SE_e, the power levels in the enclosure are monitored by a small probe placed on one of the enclosure wall. Hence, large reflection at the antenna terminal can occur due to the mismatch between the probe and the coaxial cable used to deliver the field to the probe terminal. In order to circumvent this drawback, a correction of the SE_e is accomplished. As matter of fact, two separate calibrations were performed (in the continuous stirring chamber case): a transmission one and a reflection procedure. The two measurements are taken in two separate steps. Hence, the scattering coefficients $\dot{S}_{21}$ and $\dot{S}_{22}$ are measured. Port1 is permanently connected to the horn antenna in RC. Port2 is in succession connected to the horn antenna in RC (horn-horn, hh) and to monopole antenna on the enclosure wall (horn-monopole, hm) according to Fig.1. Therefore, SE_e is achieved as follows

$$\mathrm{SE_e} = \left\langle \left|\dot{S}_{21}\right|^2 \right\rangle_{hh} - \left\langle \left|\dot{S}_{21}\right|^2 \right\rangle_{hm} + \left(1 - \left|\left\langle \dot{S}_{22} \right\rangle\right|^2\right) \qquad (11)$$

All the terms in eq. (11) are taken in dB values.

This correction has been accomplished to avoid the strong mismatch error affecting measurements that have been accomplished in the RC of the IUN. It is a 8 m^3 metallic chamber wherein three mechanical stirrers are present. The first one (S1), placed on the left of the entrance door, has a rectangular shape of 1.84mx0.45m size; the second stirrer (S2) and the third stirrers (S3) have a Greek-cross shape. S2 has bars of 1.84mx0.25m size; it is placed in front of the entrance door. The S3 stirrer has bars of 1.20mx0.18m size and it is placed in the ceiling. The S1, S2 and S3 stirrers work in continuous mode with a maximum speed of 190, 390 and 320 rate per minute (rpm), respectively. In Fig. 2 a sketch of the inner of the IUN RC with a particular of the enclosure employed in the measurements, is shown.

In all experiments the transmitting and the receiving antenna used in the RC are both Ets-Lindgren double-ridged waveguide horn certified to work in the 1 – 18 GHz frequency range. An Agilent Technologies Vector Network Analyzer (VNA) is used in experimental tests. Measurements by shifting the measuring frequency in the designed frequency range (1 – 18 GHz) by steps of 200 MHz are accomplished. 3000 independent samples are acquired at each frequency point. It must be noted that the statistically independence of the acquired samples, provided by the vibration of IUN RC walls that add up to the mechanical stirring, has been verified by the autocorrelation function (not shown to save space). The scattering coefficient S_{21} is measured and an off-line data analysis is accomplished. The software used to acquire and to off-line analyze the data is developed in LabVIEW, a graphical development environment of the National Instruments (NI).

In order to validate the theoretical model with the proposed procedure, two different-size enclosures of metallic grid, have been employed. Both the enclosures are cubic boxes of 49 cm side size. The first enclosure is made with metallic grid and its mesh size is 5 mm, see Fig. 3; the second is made with metallic fabric and its mesh size is 1 mm: the latter has a foam structure as a support, see Fig. 2. They have been placed on foam support within the RC during the measurements; the clearance from the chamber floor is 50 cm. This approach is essentially a nested RC. The stirrers within RC accomplish the randomization of the electromagnetic field. Hence, the uniformity and isotropy of the field inside the enclosure can be assumed since it is uniformly and randomly excited from all sides. In any case, when SE_e values increase until 10 dB about, a conventional stirrer must be placed within the enclosure; by experience, this concept is very more stringent for monopole mismatch measurements. It is important to note that for such measurements the enclosure is excited by monopole itself and that for the frequency points where the mismatch is very strong, the residual error about S_{22} parameter, can significantly affect the achieved SE_e, see eq. (11).

The losses inside the enclosure reduce the impedance mismatch of the probe monopole. In any case, if the assumed hypothesis of uniformity and isotropy of the field deteriorates, then the quality of expected results deteriorates as well. In particular, this problem occurs at lower frequencies in the employed frequency range, where the modal behavior of the enclosure is not negligible.

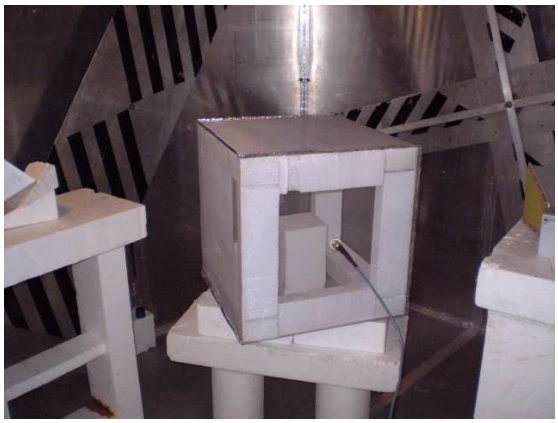

Figure 2: A sketch of the IUN RC with a particular of the enclosure made with mesh size of 1 mm.

In Fig. 4 is shown the SE_e obtained with the enclosure made with a mesh size of 5 mm. The SE_e of the enclosure with the correction due to mismatch of the probe (blue line) and without it (black line) is shown. As expected, according to the theoretical model, the SE_e shows a decreasing behavior with the frequency. It must be noted that when the black and blue line have the same value, i.e. around 3 GHz and from 6 to 8 GHz, the return loss on the receiving antenna is always smaller than 10 dB, see Figure 5.

Figure 3: 5 mm metallic mesh enclosure used for the experiments.

A visual comparison with the results obtained in [9] shows a value of SE_e smaller than SE, to witness that a shielding reduction is obtained when an enclosure is employed.
In Fig. 6 is shown the SE_e obtained with the enclosure made with a mesh size of 1 mm.

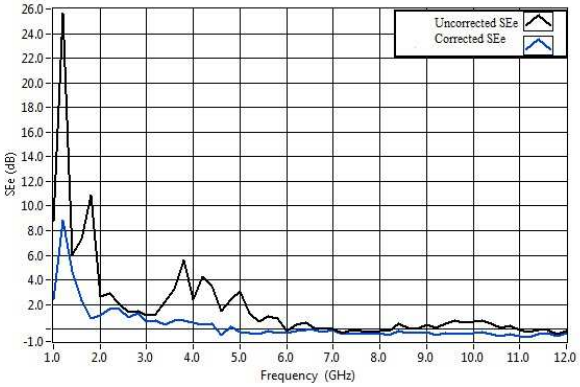

Figure 4: SE_e from measurements of 5 mm mesh size enclosure.

In conclusion, the SEe of an enclosure with wall of metallic grids decreases with the increasing of the frequency. Moreover, the SE_e is smaller than the corresponding one obtained with the same material of which the enclosure is made [9]. The SE_e of an enclosure tends to the one of a metallic grid if a load is placed within the enclosure, see next Figs. 8 and 9 in section 4.
In Fig.7 is shown a comparison between the shielding effectiveness of the enclosure made with metallic mesh of 1 mm with a piece of absorber (blue line) and without it (black line).

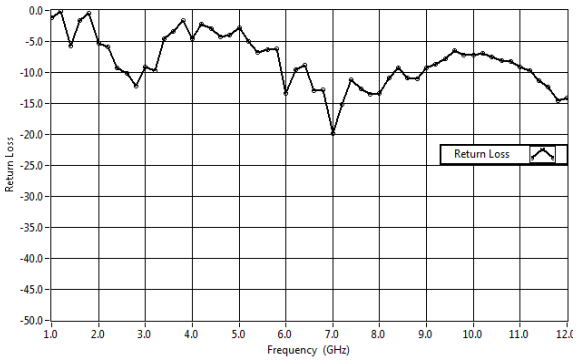

Figure 5: Return Loss, enclosure built with metallic mesh whose side is 5 mm.

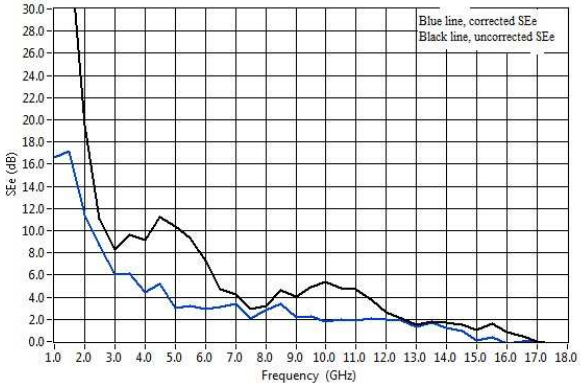

Figure 6: SE_e from measurements of 1 mm mesh size enclosure.

The absorber is of the Emerson-Cuming, its dimensions are 9 cm x 9 cm x 9 cm, and it is place on a foam support, see Fig.3. As expected, the loading effect improves the SE_e of the enclosure that increases from 2 to about 10 dB. In particular, apart from the effect due to the mismatch of the monopole, at lowest frequency, σ_t becomes smaller than $\sigma_{ae,i}$; also, $\sigma_{w,i}$ is negligible with respect to σ_t, but it has no zero value.

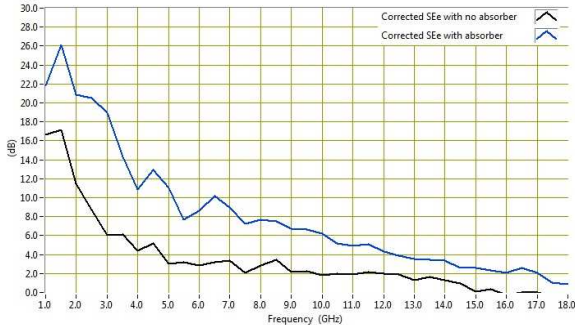

Figure 7: Enclosure made with metallic mesh of 1 mm side dimension. Difference between the SE_e with the absorber (blue line) and without it (black line) inside the enclosure.

4. Comparisons and Discussion

In this Section, the comparison between the expected results of SE_e and the measured ones is discussed. The former are achieved according to (8)-(10); the experimental measurements of R (SE), reported in Figs. 8 and 9, are the same as in [9]. One specifies that those measurements were available for the paper, and that the frequency step is 1 GHz. However, in [9] SE was simply achieved as 1-R (so it turned out to be less than 1), while it here is calculated according to (10), by estimating $\sigma_{a,gA}$, and $\sigma_{w,i}$; the latter was estimated as specified below. For the enclosure with mesh size of 5 mm, the expected SE_e is about zero dB over the whole frequency range from 1 to 18 GHz. This agrees well with experimental results in Fig. 4, in particular from 2 GHz up. Fig. 10 shows the expected results for $\sigma_{w,i}+A_e$ (black line) and $\sigma_{w,i}$ (blue line). In Fig. 11 SE_e for the enclosure with mesh size of 1 mm is shown. The calculation of A_e takes into account the developing of the model (6) [7].

The estimate of $\sigma_{w,i}$ has been simplified; indeed, it has been estimated by considering the solid part of inner total area of the wall enclosure. Clearly, the losses have been estimated by considering a field uniform and isotropic [7], [10]. For the enclosure with mesh size of 1 mm, the ratio between solid area and surface total area is equal to 0.6, and the metal type is aluminum. $\sigma_{w,i}$ has been estimated by means of the average absorption coefficient of the solid part of the enclosure walls. In other words, the solid area of inner total area of the enclosure is assimilated to a metallic plate with equivalent surface area. For a metallic plate with ordinary thickness one can write:

$$\alpha(\theta) = 1 - \frac{1}{2}\left(\left|\rho_v(\theta)\right|^2 + \left|\rho_h(\theta)\right|^2\right) \tag{12}$$

where $\alpha(\theta)$ is the absorption coefficient; $\rho_v(\theta)$ and $\rho_h(\theta)$ are the reflection coefficients, the subscripts v and h mean that the polarization is vertical and horizontal, respectively; θ is the incidence angle. In [13], under the assumed field hypothesis, it is shown that the term

$$\alpha = \int_0^{\pi/2} \alpha(\theta)\cos(\theta)\sin(\theta)d\theta \ , \tag{14}$$

which represents the average absorption coefficient of the solid part, can be expressed in the following analytical form:

$$\begin{aligned} \alpha &= \frac{4}{3}\delta k_0 + \frac{1}{2}\left(\delta k_0\right)^2 \ln\left(\frac{\left(\delta k_0\right)^2}{2}\right) \cong \frac{4}{3}\delta k_0 \\ &= \frac{4}{3}\sqrt{\frac{4\pi\varepsilon_0 f}{s_w}} \end{aligned} \tag{15}$$

where k_0 is the free-space wavenumber, δ is the skin depth, f is the frequency, s_w is the conductivity of the metal forming the grid or the fabric, ε_0 represents the free-space permittivity.

In short, by also considering (10), one can write:

$$\sigma_{w,i} = \left(\frac{4}{3}\sqrt{\frac{4\pi\varepsilon_0 f}{s_w}}C_1 2\right)\sigma_{a,gA} = \left(1 - R_{w,i} - \frac{1}{SE}\right)\sigma_{a,gA} \tag{16}$$

where C_1 is a constant equal to the ratio between solid area and surface total area. (16) has been used to estimate $\sigma_{w,i}$.

For the enclosure with mesh size of 1 mm, $C_1 = 0.6$, as said above, and s_w=3.8e+7 S/m.
By considering (10) and the results in Figs. 8 and 10, it can be noted that $\sigma_{w,i}$ has a negligible effect on SE of a metallic fabric with mesh size of 1 mm as well, and that A_e can have a significant effect on SE_e at low frequencies.

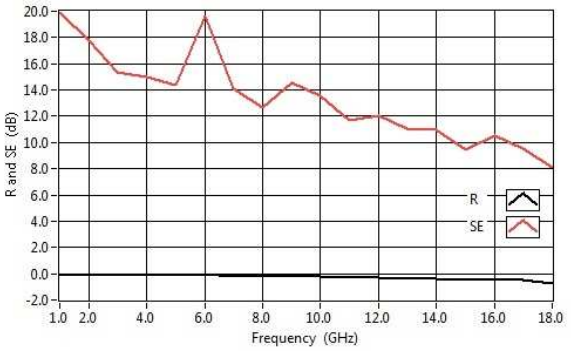

Figure 8: Reflectivity (black line) and SE (red line) vs. frequency of a 1 mm side dimension mesh grid.

Results in Fig. 11 shown that the expected SE_e appreciably differs from measured one from 1 to 5 GHz, and the result mismatch decreases as the frequency increases. The authors think that the mismatch of the results at lower frequencies in the employed frequency range is due to the fact that the modal behavior of the enclosure is not negligible, so that the necessary property of uniform and isotropy of the field are no more fully satisfied.
Uniformity and isotropy of the field can be improved by a mechanical stirred installed inside the enclosure; however, at frequencies where the modal density is inadequate, it is not possible to obtain field uniformity and isotropy within the enclosure.

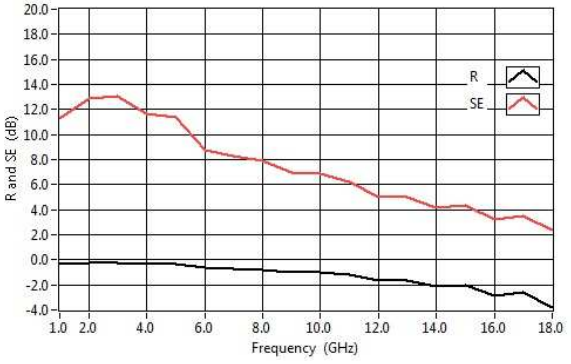

Figure 9: Reflectivity (black line) and SE (red line) vs. frequency of a 5 mm side dimension mesh grid.

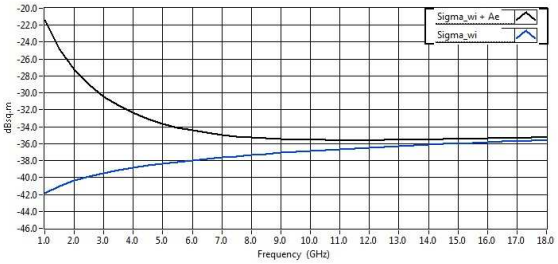

Figure 10: Expected results in dBsq.m. for $\sigma_{w,i}$+A_e (black line) and $\sigma_{w,i}$, (blue line) for the enclosure with mesh size of 1 mm

Different conditions of field affect the estimate of all the parameters in (4); that is, both the estimate of $\sigma_{w,i}$ and A_e would turn out to be affected; however, at lower frequencies the effective area of the monopole is significantly greater than $\sigma_{w,i}$, and it can assume appreciably values higher from the expected ones. Also, at the frequency points where the mismatch is very strong, the correction in eq. (11) can turn out been affected. Finally, another reason for mismatch of the results can be the accuracy of the R (SE) measurements.

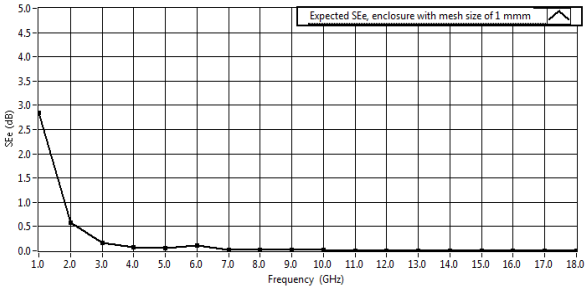

Figure 11: Expected SE_e for the enclosure with mesh size of 1 mm

Both models (2) and (7) have been developed under conditions of uniformity and isotropy of the field; in principle, they could be applied in different field conditions as well; but that is very difficult, as the estimates of the parameters requires the accurate knowledge of the field structure inside an enclosure.
It is well known that the leakage for an enclosure can be low, but it cannot be zero. Therefore, it is important to note that an enclosures must be made with material having both high SE and low R [11], where the latter refers to internal side of the enclosure walls.

5. Uncertainty Measurements

When SE_e is equal to about 0 dB, a slightly negative value can be measured, as it can be clearly noted in Figs. 4. It is due to imperfect field isotropy and uniformity, which causes a measurement uncertainty. The field conditions of uniformity and isotropy depend on effectiveness of the stirrers; for our RC used in the experiments, a field uniformity within ±0.5 dB was measured at 1 GHz with unloaded chamber [12]. This already justifies the SE_e slightly negative which has been measured.
In any case, for further information, an estimate of the SE_e overall measurement uncertainty is here performed, by measuring it in 10 different configurations of the measurement setup. Each independent measurement configuration is achieved by changing the location of the enclosure and/or horn antennas and/or their polarization. The results are shown in Figs. 12 and 13, where are illustrated SE_e uncorrected and corrected, respectively. In order to save time, 1000 independent samples are acquired at each frequency point, in a frequency range from 1 GHz to 12 GHz with step frequency of 200 Mhz.

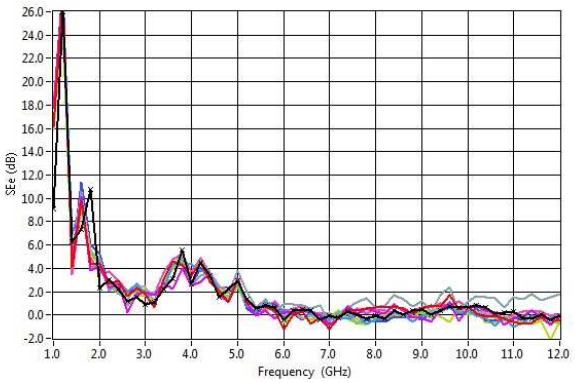

Figure 12: Uncorrected SE_e from measurements of 5 mm mesh size enclosure; 10 independent measurement configurations; 1000 independent samples at each frequency point.

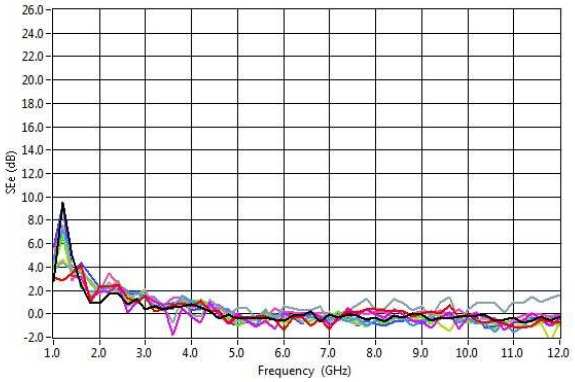

Figure 13: Corrected SE_e from measurements of 5 mm mesh size enclosure; 10 independent measurement configurations; 1000 independent samples at each frequency point.

Therefore, the standard deviation of SE_e is estimated for 10 independent measurement configurations. Fig. 14 shows the standard uncertainty [14] of corrected SE_e; the standard uncertainty (in dB) is expressed relative to the mean. It is important note that the standard uncertainty was estimated in conditions absolutely realistic; that is, it was actually calculated in the same conditions of measurement (with enclosure inside the chamber). The estimated uncertainty includes the degrade of the calibration of the VNA which due to the repeated connections which were necessary between a measure and the other (two-port VNA) and the time taken to make the measures. This in particular affects the mismatching measurements, as one can note in Figs. 12, 13 and 14. In fact, a high deviation of the SE_e is noted at 1.2 GHz for corrected results only.

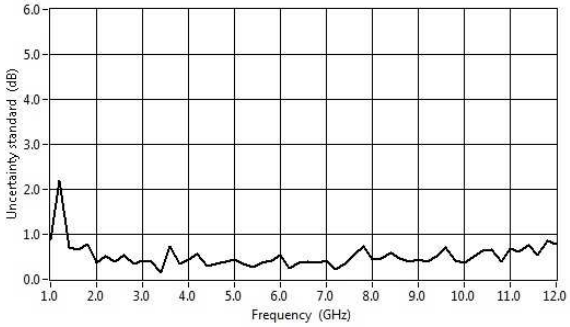

Figure 14: Standard uncertainty of corrected SE_e in dB

On the other hand, the monopole probe is strongly mismatched at that frequency, see Fig. 5 as well. It is specified that the tests were performed on a time of six hours about included warm-up and calibration procedure. However, the max of the standard uncertainty of SE_e is less than 1 dB, except the value of 2.2 dB at 1.2 GHz. The estimate uncertainty is conservative with respect to the measures shown in Fig. 4, where 3000 points are acquired for each frequency, and because it is based only on 10 independent measurement configurations; moreover it includes the degrade of the calibration as specified above. However, it is consistent with results shown in [12] and is adequate to the experience and confirms the conclusions drawn here.

6. Conclusions

In this paper a different form of the SE_e of an enclosure made with metallic grids has been proposed and successfully tested by measurements accomplished at IUN RC. Measurements have been accomplished for the first time on enclosure totally made with square metallic mesh and they have been proved that the SE_e of an enclosure is always smaller than the SE of a material. Further, the SE_e of such enclosures is decreasing with the increasing of

frequency. Finally, by loading the enclosure with absorbing material, it has been noted that the SE_e tends to the one of the wall metallic grid.

Acknowledgement

The authors thank Mr. Giuseppe Grassini of the Electrical and Electronic Measurements Lab (at Department of Technology, University of Napoli Parthenope) for helping in conducting the experiments that have been used in this paper.

References

[1] C. L. Holloway, D. A. Hill, M. Sandroni, J. M. Ladbury, J. Coder, G. Koeple, A. C. Marvin, and Y. He, "Use of revereration chambers to determine the shielding effectiveness of physical small, electrically large enclosures and cavities," *IEEE Trans. On. Electromag. Compatibility*, Vol. 50, No. 4, pp. 770-782, 2008.

[2] D. A. Hill, M. T. Ma, A. R. Ondrejka, B. F. Riddle, M. L. Crawford, and R. T. Johnk, "Aperture excitation of electrically large, lossy cavities," *IEEE Trans. On. Electromagn. Compatibility*, Vol. 36, No. 3, pp. 169-178, 1994.

[3] C. L. Holloway, D. A. Hill, J. Ladbury, G. Koepke, R. Gracia, "Shielding effectiveness measurements of materials using nested reverberation chamber," *IEEE Trans. On. Electromag. Compatibility*, Vol. 45, No. 2, 350-356, 2003.

[4] K.F.Casey, "Electromagnetic shielding behavior of wire mesh screens", *IEEE Trans. On. Electromag. Compatibility*, Vol. 30, No. 3, pp.298-306, 1988.

[5] V. M. Primiani, F. Moglie, A. P. Pastore, "Field penetration through a wire mesh screen excited by a reverberation chamber field: FDTD analysis and experiments", *IEEE Trans. On. Electromag. Compatibility*, Vol. 51, No. 4, pp.883-891, 2009.

[6] A. Gifuni, M. Migliaccio, "Used of nested reverberating chambers to measure shielding effectiveness of nonreciprocal samples taking into account multiple interactions", *IEEE Trans. On. Electromag. Compatibility*, Vol. 50, No. 4, pp. 783-786, 2008.

[7] A. Gifuni, "Relation between the shielding effectiveness of an electrically large enclosure and the wall material under ideal field conditions," submitted to *IEEE Trans. On Electromagnetic Compatibility* .

[8] A.Gifuni, "On the measurement of the absorption cross section and material reflectivity in a reverberation chamber," *IEEE Trans. Electromagn. Compat.,* vol.51, pp. 1047-1050, 2009.

[9] A. Gifuni, A. Sorrentino, G. Ferrara, M. Migliaccio, A. Fanti, G. Mazzarella, "Measurements on the Reflectivity of materials in a reverberating chamber", *Proceeding on Antenna and Propagation Conference* (LAPC), pag.1-4, 2011.

[10] D. A. Hill, "A reflection coefficient derivation for the *Q* of a reverberantion chamber," *IEEE Trans. Electromagn. Compat.*, vol.38, pp.591-592, November 1996.

[11] N. F. Colaneri and L. W. Shacklette, "EMI shielding measurements of conductive polymer blends," *IEEE Trans. Instrum. Meas.*, vol.41, pp.291-297, April 1992.

[12] P. Corona, G.Latmiral, and E.Paolini, L. Piccioli, "Use of reverberating enclosure for measurements of radiated power in the microwave range", *IEEE Trans. Electromagn. Compat.*, vol.18, pp. 54-59, May 1976.

[13] A. Gifuni, "Calcolo delle perdite elettromagnetiche nelle pareti delle camere riverberanti", Università degli studi di Napoli "Parthenope", Dipartimento per le Tecnologie, Napoli 2004.

[14] B.N. Taylor and C.E. Kuyatt, "Guidelines for evaluating and expressing the uncertainty of NIST measurement results, "NIST Tech. Note 1297, Sept. 1994.